Desalination and Water Treatment
www.deswater.com

doi: 10.5004/dwt.2020.25831

193 (2020) 224–234
July

Modeling of fluoride rejection from aqueous solution by nanofiltration process: single and binary solution

Ali Fatehizadeh[a,b], Mohammad Mehdi Amin[a,b], Mika Sillanpää[c,d,e], Nahid Hatami[b,f], Ensiyeh Taheri[a,b,*], Najmeh Baghaei[b,f,*], Shreya Mahajan[g]

[a]*Environment Research Center, Research Institute for Primordial Prevention of Non-Communicable Disease, Isfahan University of Medical Sciences, Isfahan, Iran, Tel. +98 31 3792 3296; Fax: +98 31 3792 5849; emails: e_taheri_83@yahoo.com (E. Taheri), a.fatehizadeh@hlth.mui.ac.ir (A. Fatehizadeh), amin@hlth.mui.ac.ir (M.M. Amin)*
[b]*Department of Environmental Health Engineering, School of Health, Isfahan University of Medical Sciences, Isfahan, Iran, Tel. +98 31 3792 3277; emails: najmeh.b.1997@gmail.com (N. Baghaei), na.hatami123@gmail.com (N. Hatami)*
[c]*Institute of Research and Development, Duy Tan University, Da Nang 550000, Vietnam, email: mikaesillanpaa@gmail.com (M. Sillanpää)*
[d]*Faculty of Environment and Chemical Engineering, Duy Tan University, Da Nang 550000, Vietnam*
[e]*School of Civil Engineering and Surveying, Faculty of Health, Engineering and Sciences, University of Southern Queensland, West Street, Toowoomba, 4350 QLD, Australia*
[f]*Student Research Committee, School of Health, Isfahan University of Medical Sciences, Isfahan, Iran*
[g]*Department of Chemistry, Dr. B.R. Ambedkar National Institute of Technology, Jalandhar 144011, Punjab, India, email: mahajanshreya219@gmail.com (S. Mahajan)*

Received 29 July 2019; Accepted 12 March 2020

ABSTRACT

This study was aimed at the investigation of fluoride (F^-) rejection from single and binary solution by nanofiltration process (NF). The influence of various parameters such as the effect of solution pH, initial F^- concentration, applied pressure, feed flux, and accompanying cations and anions in feed water has been reported. Besides, the solute rejection and Spiegler–Kedem models were applied for the better understanding of NF performance. In a single solution, the laboratory study demonstrated F^- rejections with NF membranes to be higher than 85%. Moreover, as applied pressure and feed flux increased F^- rejection was observed to increase marginally whereas the opposite trend was observed when initial F^- concentration in feed water was increased. Further, the depletion of F^- rejection at 15 mg/L of F^- was found to be associated with the presence of co-existing cation and anion in the feed water. The estimated average of pore radius and $\Delta x/A_k$ of the NF membrane were 0.12 ± 0.02 nm and 47.84 ± 25.22 mm, respectively.

Keywords: Fluoride rejection; Cost evaluation; Drinking water; Membrane modeling; Nanofiltration

1. Introduction

One of the widely distributed elements in Earth's crust is Fluorine (F^-) which is found in the forms of mineral such as fluorspar, cryolite, and fluorapatite [1]. Despite the fact that centers for disease control and prevention acclaims the fluoridation of drinking water as one of the 10 key public health accomplishments of the 20th century's, but the World Health Organization has classified the F^- as one of the significant water contaminants that leads to adverse health effects in humans when present in an exorbitant amount in drinking water [2].

* Corresponding authors.

The effect of fluoride in drinking water can be advantageous or deleterious to mankind. The deciding parameters are concentration and the duration of uptake. Therefore, when present in a narrow concentration range, it plays an imperative role in the mineralization of bones and also acts as an antibacterial agent in the mouth. On the contrary, excess concentration (3–6 mg/L) of fluoride can have an adverse effect on bones and dental (dental and skeletal fluorosis) [3]. According to the US environmental protection agency, the maximum fluoride contaminant level and secondary maximum contaminant level values should be 4 and 2 mg/L, respectively. However, according to the national standard of Iran, the range of fluoride content in drinking water should be 0.5–1.5 mg/L [4,5].

Different concentrations of F^- is present in a diverse type of water bodies, but the higher concentrations are reported for groundwater [1].

Iran is located in a semi-arid area with an average annual precipitation of less than one-third of that of the world [6]. In 2011, approximately 98.4% of the urban population of Iran were served by public water systems and the portions of surface and groundwater resources in the water supply were 33% and 67%, respectively [7]. Previous studies showed the F^- concentration in the groundwater resources of Iran was ranging from 0.11 to 6 mg/L [8,9]. The high F^- concentration of groundwaters in Iran is associated with calcium and magnesium bicarbonate ($Ca(HCO_3)_2$ and $Mg(HCO_3)_2$) type of water [7]. Hence, in this direction, over the years, the plethora of conventional methods have been implemented for the defluoridation of water namely adsorption, ion exchange, precipitation–coagulation, and membrane-based processes [10]. Among them, coagulation–precipitation is the most common, effective, widespread, and cheap method for fluoride removal from drinking water. Despite its advantages, the major issue associated with this technique is the generation of harmful waste products. Similarly, the ion exchange and membrane process which is mainly the reverse osmosis (RO) technique requires high maintenance cost due to fouling, scaling, and degradation of membrane [11]. Therefore, the most efficient one, in practice, for the defluoridation is adsorption due to its advantages such as its simplicity, effectiveness, and economic viability [12].

Furthermore, among the membrane processes, nanofiltration (NF), one of the modern technologies, has attracted immense attention owing to its wide array of applications particularly for drinking water and wastewater treatment. This process operates between reverse osmosis (RO) and ultrafiltration (UF) properties and it is symbolized as a softening membrane because it was basically developed for softening [13].

After the development of RO membranes in the seventies, the relatively high energy cost lead to the development of advanced and improved membranes with lower rejections of dissolved components and higher water permeability. As a result, the "low-pressure reverse osmosis membranes" known as NF membranes was established and utilized in the second half of the eighties [14]. Besides, NF, as compared to RO, operates at lower pressure by the same permeate flux efficiency. Also, by application of NF for water defluoridation, the optimum F^- concentration can be achieved by adjusting the operation conditions [15].

Previous studies reported, NF system to be acceptable in defluoridation groundwater at a low cost thus making it economically and operationally attractive [16]. Besides, the NF membranes based on operation condition and modifications have different rejection efficiency with more than 80% rejection efficiency of F^- [16–18].

The previous studies have reported the usage of "dense" NF membrane such as NF70 and NF90 and "loose" NF membrane including NF270, NF400, and TR60 for F^- retention from model solutions [13,19]. Nasr et al. [20] compared the performances of two commercial NF membranes (NF5 and NF9) for F^- rejection from groundwater. The authors also showed that with the application of NF5 and NF9 membrane, the F^- concentration in permeate was observed to be 1.45 mg/L (F^- retention: 57%) and 0.38 mg/L (F^- retention: 88%), respectively. According to previous studies, the "dense" NF membrane is recommended for surface and groundwater treatment because it removes a high percentage of salts and organics whereas the "loose" NF membrane is appropriate in those water treatment where only good organic rejection is desired with partial softening [21].

Since the separation mechanism of the NF membranes is very complicated, several models were established to illustrate and foresee the flux and the retention of a variety of species under different operating conditions. The proposed models can be allocated into three classes, that is: irreversible thermodynamics models, pore models, and non-porous (homogenous) models [22]. Usually, characteristics of the NF membrane such as pore size, effective thickness to porosity ratio, and the membrane charge density are assessed by solutes (uncharged) and salts rejection experiments by employing pore models like Donnan steric partitioning pore model, steric hindrance pore model, or more complex Donnan steric pore model and dielectric exclusion. The aforementioned models can also be utilized for determining the performances of distinct processes only if the attributes of the membranes applied are known [23].

Presently, the retention mechanism of the NF membrane process is complicated and not yet fully known. Extensive work has been done and is still being conducted to investigate transfer and retention mechanisms including NF processes modeling. The many models were constructed to describe and predict the flux and retention of various charged and uncharged species by NF membrane and can be used for the determination of membrane characteristics including effective thickness to porosity ratio, pore size, and membrane charge density, and prediction of the NF processes performance.

Considering the risk of groundwater consumption with a high concentration of F^- and also with the complexity and rejection potential of the NF process, investigations on efficient NF membranes and a whole understanding of membrane performance and separation mechanism in F^- rejection by NF are of utmost interest. The main aim of this study was to determine the NF membrane efficiency on F^- rejection. Furthermore, the effects of operational parameters including solution pH, initial F^- concentration, applied pressure, feed flux, and presence of co-existing cations and anions in feed water were thoroughly investigated. The processes were characterized by using the Spiegler–Kedem model to ascertain reflection coefficient (σ) and

solute permeability (ω) parameters, and the membrane transport parameters determined from the permeation data were used to demonstrate the transport mechanism. In addition, the economic evaluation was conducted to assess the real costs of NF membrane process.

2. Materials and methods

2.1. Nanofiltration set up

All the experiments were carried out by the NF pilot plant (NF90) supplied by FILMTEC™ membranes (Dow Chemical Company, USA). The properties of NF membranes are summarized in Table 1.

The experiments were performed with a crossflow separation unit as shown schematically in Fig. 1. The applied pressure over the membrane can be varied from 5 to 8 bar with manual pressure valves. The NF system equipped with a spiral wound membrane of 0.05 m internal diameter and 0.24 m length, the effective membrane filtration area being 0.22 m^2. In addition, the NF system consisted of barometer and feed tank with 10 L effective volume.

2.2. Experimental procedure

Before experiments, in order to remove preservatives, the NF membrane was soaked in the deionized water for 48 h and rinsed with deionized water until the conductivity of permeate remained below 1 mS/cm. The feed solution was pumped from a feed tank, through NF membrane and back to the reservoir. The pump (Aqua Care Co., Ltd., Taiwan) provided pressure up to 9.5 bar and flow rate up to 1.6 L/min. The experiments were carried out under the various solution chemistries included solution pH (3–8) and initial F^- concentration (5–30 mg/L) in total recirculation mode. In this operation mode, both the concentrate and the permeate streams were recirculated into the feed tank, thus the feed concentration was kept approximately constant. The pure water flux (J_w) was measured at different transmembrane pressures in 4–8 bar range, and the membrane pure water permeability (LP) was calculated. After each experiment, the system was cleaned with demineralized water for 3 h at 5 bar, until the water flux and permeability of the membrane were restored.

2.3. Chemicals and instrumentation

All the reagents used in the experiments were of analytical reagent grade. A standard stock solution of 1 g/L of F^- was prepared using NaF (Merck Co., Germany) dissolved in deionized water and was stored in a dark

Table 1
Characteristics of NF membranes

Item	Description
Membrane type	Spiral wound
Material	Polyamide
Cut off (Da)	90
Surface (cm^2)	480
Membrane surface charge	Negative
Feed pH range	1.5–10.5
Operating pressure (bar)	0–60
Operating temperature (°C)	0–70

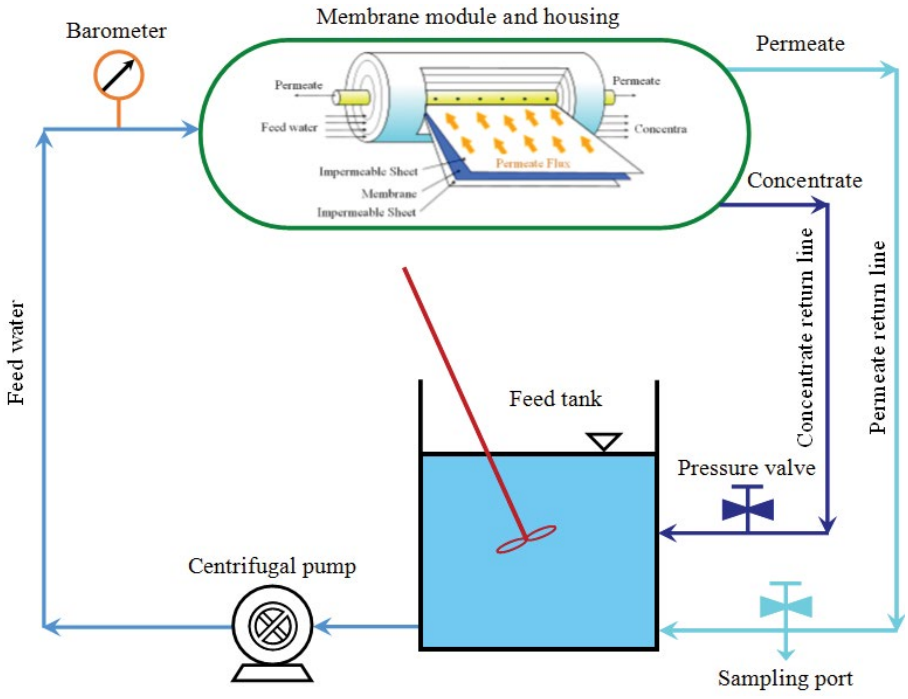

Fig. 1. NF pilot plant diagram.

glass container and kept in the refrigerator at 5°C–8°C. The binary solution experiments were carried out with NaCl, $CaCl_2{\cdot}2H_2O$, Na_2SO_4, and NaH_2PO_4 (Merck Co., Germany) salts. To obtain the desired F^- concentration, the stock solution was diluted in demineralized water and the pH of the solution was maintained using 0.1 M of HCl or NaOH. The F^- concentration was measured using the sodium 2-(parasulfophenylazo)-1,8-dihydroxy-3,6-naphthalenedisulfonate (SPADNS) reagent and the color loss was measured at 570 nm by DR5000 spectrophotometer (Hach Lange GmbH, Germany) [24]. Before F^- analysis, the solution pH of samples was adjusted to 5 ± 0.1 with acetate buffer solution.

2.4. Calculation

2.4.1. Nanofiltration transport and concentration polarization

The observed F^- rejection was calculated with measuring the F^- concentrations in feed and permeates solution according to Eq. (1).

$$R_0 = \left(1 - \frac{C_{i,p}}{C_{i,f}}\right) \times 100 \tag{1}$$

Based on the film model, the intrinsic rejection of the membrane with considering the effect of the concentration polarization phenomenon is calculated by Eqs. (2) and (3).

$$C_{i,m} = C_{i,p} + \left(C_{i,f} - C_{i,p}\right) \times \exp\left(\frac{J}{k}\right) \tag{2}$$

$$R_0 = \left(1 - \frac{C_{i,p}}{C_{i,m}}\right) \times 100 \tag{3}$$

By applying the Sherwood relationship with Deissler correlation (Eq. (4)), the permeate volume flux (J) and mass transfer coefficient (k) in Eq. (2) can be computed [25].

$$\mathrm{Sh} = 0.023 \times \mathrm{Re}^{0.875} \times \mathrm{Sc}^{0.25} \tag{4}$$

In Eq. (4), the Reynolds (Re), Schmidt (Sc), and Sherwood (Sh) numbers were calculated by Eqs. (5)–(7), respectively.

$$\mathrm{Re} = \frac{u \times \rho \times d_h}{\eta} \tag{5}$$

$$\mathrm{Sc} = \frac{\eta}{\rho \times D_{i,\infty}} \tag{6}$$

$$\mathrm{Sh} = \frac{k \times d_h}{D_{i,\infty}} \tag{7}$$

Cavaco Morão et al. [26] presented the NF membranes modeling with bundles of slit-like pores with the length Δx and the half-width r_p. In this case, considering steric effects, the rejection is determined by fitting of the pore radius and the thickness/porosity ratio by Eq. (8).

$$R = \left(\frac{\phi_i \times K_{i,c}}{1 - \left[\left(1 - \phi_i - K_{i,c}\right) \times \exp\left(-\mathrm{Pe}\right)\right]}\right) \tag{8}$$

In Eq. (8), the Peclet number (Pe) is defined as Eq. (9) [26].

$$\mathrm{Pe} = \left(\frac{K_{i,c} \times J}{K_{i,d} \times D_{i,\infty}}\right) \times \left(\frac{\Delta x}{A_k}\right) \tag{9}$$

For slit-like pores, Dechadilok and Deen established equations for calculation of hindrance factors according to Eqs. (10)–(15) [27].

$$\lambda_i = \frac{r_{i,s}}{r_p} \tag{10}$$

$$\phi_i = 1 - \lambda_i \tag{11}$$

$$H(\lambda_i) = 1 + 0.5625\lambda_i \ln\lambda_i - 1.19358\lambda_i + 0.4285\lambda_i^3 - 0.3192\lambda_i^4 + 0.8428\lambda_i^5 \tag{12}$$

$$K_{i,d} = \frac{H\left(\lambda_i\right)}{\phi_i} \tag{13}$$

$$W(\lambda_i) = 1 - 3.02\lambda_i^2 + 5.776\lambda_i^3 - 12.3675\lambda_i^4 + 18.9775\lambda_i^5 - 15.2185\lambda_i^6 - 4.8525\lambda_i^7 \tag{14}$$

$$K_{i,c} = \frac{W(\lambda_i)}{\phi_i} \tag{15}$$

By measuring water flux and applying Hagen–Poiseuille equation, for slit-like pores, the thickness to porosity ratio is calculated with Eq. (16) [26].

$$J_w = L_p \times \Delta P = \left(\frac{r_p^2}{3 \times \mu \times \left(\Delta x / A_k\right)}\right) \times \Delta P \tag{16}$$

In the case of NF and RO processes, the solvent and single solute transport are described with irreversible thermodynamics in the Spiegler–Kedem model. In this model, solvent and solute transport is related to the sum of diffusive because of concentration difference at the membrane sides and convective due to the pressure gradient of flux. Eqs. (17) and (18) present the Spiegler–Kedem model [28].

$$R = \frac{\sigma(1 - F)}{1 - \sigma F} \tag{17}$$

$$F = \exp\left(-\frac{1 - \sigma}{\omega} \times J_p\right) \tag{18}$$

2.4.2. Economical evaluation

To evaluate the NF membrane process economics for rejection of F^- from groundwater, the proposed method by

Verberne and Wouters [29] was used. The imperative cost determining elements in the membrane filtration installation are feeding pumps, membrane modules, pressure vessels, chemical storage and dosing, energy supplies, and pipe working. To estimate the investments for installation, the investments are linked to the feed flow rate and the number of membranes in the plant that are determined by the feed pressure of the plant. The civil and mechanical investments are related to the feed flow and the number of membranes. For the electrical investments, a function has been chosen depending on the feed flow and the feed pressure. The costs for membranes are directly linked to the number of membranes. Eqs. (19)–(29) were used to estimate the total costs of NF installation and are summarized in Table 2.

3. Results and discussion

3.1. Single solution

3.1.1. Effect of pH value on F^- rejection

The solution pH plays a significant role which not only influences the membrane charge but also the solution chemistry. The effect of solution pH ranging from 3 to 8 on F^- rejection by NF with 5 mg/L of F^- concentration (flow rate: 30 L/min and applied pressure: 5 bar) was investigated. The variation of F^- rejection by NF as a function of solution pH is illustrated in Fig. 2.

As seen in Fig. 2, with increasing solution pH from 3 to 5, the F^- rejection was observed to decrease from 91.3% to 53.3% and then promptly increased to 97.7% as solution pH reached to 8. This condition was controlled by several mechanisms including membrane pore size modification, electro-viscous effect, and osmotic pressure gradient. Furthermore, the solution pH can influence the solution chemistry and surface membrane charge [22,30]. In addition, the main rejection phenomena of NF membranes are size exclusion of uncharged solute molecules and charge exclusion (co-ion electrostatic repulsion) of ionic species [31]. According to Fig. 2, feed water with solution pH lower than 5 leads to an increase in F^- rejection. This is probably associated with increased electrostatic repulsion between the protonated amino groups [32]. As shown in Fig. 2, the F^- rejection was robustly reduced at a solution pH 5. This behavior can be explained by the fact that the isoelectric point of the NF membranes is at about pH 5. Above solution pH 5, the NF membrane is negatively charged due to dissociation of carboxyl functional and below 5 pH, the surface of the NF membrane is positively charged which is related to the protonation of amine functional groups [33]. Moreover, the hydrofluoric acid (HF) is a weak acid with pKa of 3.1, and F^- has a tendency to form neutral ion-pair clusters $F^-H_3O^+$ in weak acid dilute solutions, causing a lower fluoride (F^-) rejection by the negatively charged membrane surface [21]. Hagmeyer and Gimbel [33] demonstrated the isoelectric point of studied membranes around solution pH 4 and the dramatic reduction in Cl^- rejection was observed around 80% at solution pH of 3 to 30% at solution pH of 4 and then increased to 90% at solution pH of 6. On other hand, at low solution pH, higher retentions of species present in feed water including F^- and H^+ ions are present which increases the osmotic pressure around the membrane surface. Subsequently, the increase in osmotic pressure leads to higher F^- rejection by NF as reported by Gherasim et al. [22]. As shown in Fig. 2, F^- rejection increases from solution pH 5 to 8 this is associated with increased co-ion charge exclusion [31,33]. The membrane to be more negatively charged over at solution pH of 8 and lead to electrostatic repulsion of the membrane surface for F^- ion and will be rejected by the membrane [31].

3.1.2. Effect of initial F^- concentration

The initial F^- concentration in feed water is important in order to assess the applicability range and optimum operating conditions of the NF process. The influence of initial F^- concentration on the rejection of F^- ions by NF membrane was investigated by carrying out experiments by feed water with solution pH of 8 (as optimal solution pH) over a concentration range of 5 to 30 mg/L by the transmembrane pressure of 5 bar at a flow rate of 30 L/min. The amount of F^- rejection by NF understudied initial F^- concentration is shown in Fig. 3.

Table 2
Equation for estimation of total costs of NF installation

Cost type	Sub-cost	Equation	
Investment	(1) Civil	$55.73Q_f^* + 80.1n$	(19)
	(2) Mechanical engineering	$233.44Q_f^{0.85} + 58.75n$	(20)
	(3) Electrical	$3 \times 10^3 + (3.49 \times P^* \times Q_f)$	(21)
	(4) Membrane module	$666n$	(22)
	Total capital cost	(1) + (2) + (3) + (4)	(23)
Operating	(5) Maintenance cost	2% of total investment	(24)
	(6) Membrane	60 \$/m^2 (6 months membrane life)	(25)
	(7) Labor	400 \$/month	(26)
	Total operating cost	(5) + (6) + (7)	(27)
	CRF***	$(i^{****} \times (1 + i)^{n*****}) \div ((1 + i)^n - 1)$	(28)
The annualized capital cost (A)		(Total capital cost × CRF) ÷ Q_p******	(29)

*Q_f, feed flow rate; **P, operating pressure; ***CRF, capital recovery factor; ****i, interest rate; *****n, project life; ******Q_p, permeate production.

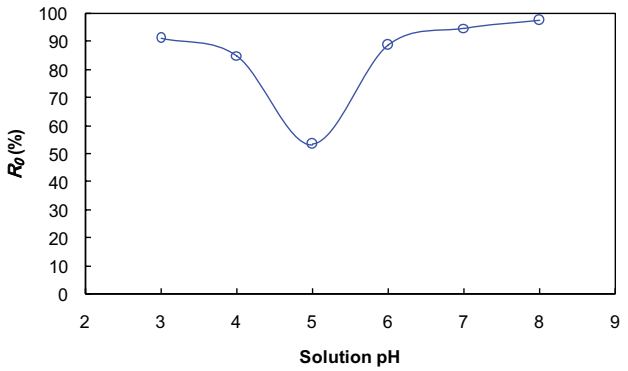

Fig. 2. Effect of solution pH on F⁻ rejection by NF (F⁻ concentration: 5 mg/L, flow rate: 30 L/min, and applied pressure: 5 bar).

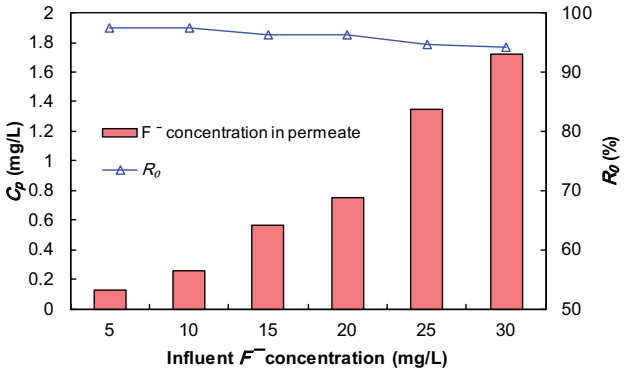

Fig. 3. F⁻ rejection as a function of initial F⁻ concentration (solution pH: 8, flow rate: 30 L/min, and applied pressure: 5 bar).

As the initial F⁻ concentration in feed water was increased from 5 to 30 mg/L, the F⁻ rejection efficiency was observed to dismiss from 97.4% to 95.2%, whereas the amount of residual F⁻ concentration in permeate showed enhancement from 0.13 to 1.72 mg/L. This behavior is allied to the characteristics of the charged membranes and known as the screen phenomenon [34,35]. With increased dissolved F⁻ in the feed water, the concentrations of Na^+ also increased. The cations neutralized the negative charges on the membrane and increased passage of the F⁻ ions through the membrane [34,36]. Kim et al. [37] reported that as the feed KCl concentration increased, chloride rejection was observed to reduce.

3.1.3. Applied pressure effect

For the treatment of F⁻ contaminated drinking water sources, the F⁻ rejection technologies must meet guidelines specific to resource-limited environments, such as restrictions regarding availability of the electricity, spare parts, and knowledgeable operators. To overcome the unavailability of electricity, this research paper examines the feasibility of treating F⁻ contaminated water with a low-pressure NF membrane. Fig. 4 shows the influence of applied pressure (4–8 bar) on the variation of F⁻ rejection with an initial F⁻ concentration of 15 ppm.

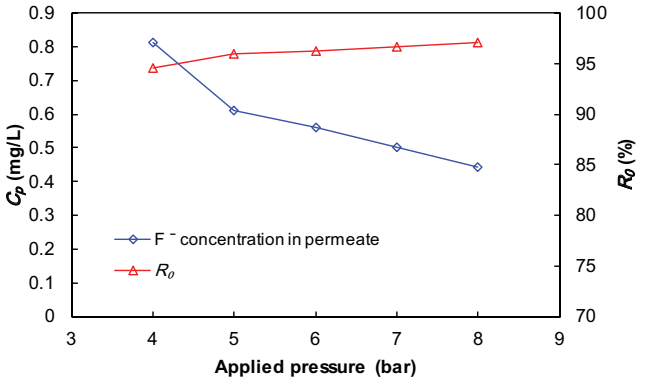

Fig. 4. F⁻ rejections under different applied pressure (F⁻ concentration: 15 mg/L, flow rate: 30 L/h, and solution pH: 8).

The F⁻ retention plots presented in Fig. 4 highlights improved F⁻ rejection efficiency during NF operation with higher applied pressure. With increasing applied pressure from 4 to 8 bar, the F⁻ rejection enhanced from 94.6% to 97.4%, however, the F⁻ concentration in permeate water reduced from 0.81 to 0.39 mg/L. In general, two different phenomena with opposite effects on the rejection are involved in ions separation under different applied pressure; first, the increasing membrane solvent flux as an function of applied pressure increases, but the ion fluxes remain unchanged because of retention of the ions by steric/charge interactions and second, concentration polarization phenomenon decreases the charge effect and thus produces an increase in the solute transfer through the membrane and consequently decreases the rejection [32,38]. Nasr et al. [20] evaluated the defluoridation of two commercial NF membranes (NF5 and NF9) and showed fluoride rejection rate increased with ascending of applied pressure.

3.1.4. Influence of feed flux

Hence, to investigate the effects of feed flux on the F⁻ separation performance of the NF membrane, the experiments were conducted under different flux ranging from 60 to 180 L/m² h with the connection of three feed pumps in parallel. Profiles of F⁻ concentration and rejection as a function of feed flux are shown in Fig. 5.

As illustrated in Fig. 5, F⁻ rejections slightly increased with increasing feed flux in the tested range. The highest and lowest F⁻ retention was achieved at 180 and 60 L/m² h and equal to 96.9% and 93.9%, respectively. The F⁻ rejection increment due to the feed flux increasing can be ascribed to the dilution effect [39]. During filtration, permeate (solution) flow and F⁻ (solute) flow are not totally coupled. Although the permeate flow increases, but the F⁻ flow remains constant, and consequently, the F⁻ concentration decreased.

One of the major drawbacks of the NF process is the concentration polarization phenomenon. Therefore, the process performance reduces when osmotic pressure is increased, as solutes accumulation is observed near the membrane on the high-pressure side. Also, the degree of mixing near the membrane surface increases as the flow rate is increased [32,37]. Thus, the concentration of solutes at the membrane

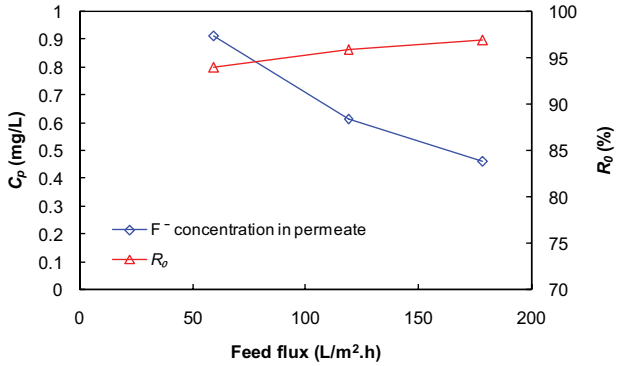

Fig. 5. Effect of feed flux on F⁻ rejections (F⁻ concentration: 15 mg/L, solution pH: 8, and applied pressure: 5 bar).

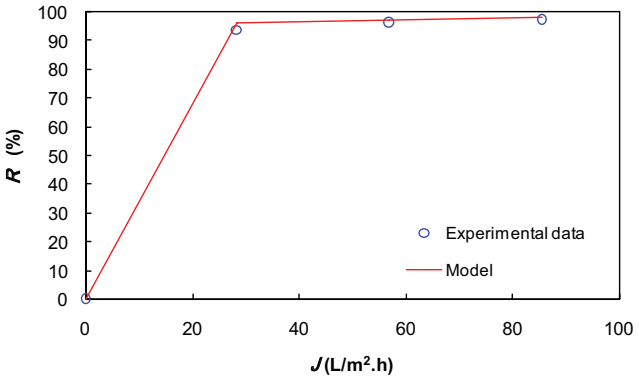

Fig. 7. Plot of the experimental and calculated rejections by fitting pore radius.

surface is higher than in the bulk of the feed, and a boundary layer thus builds as a result of the equilibrium established between the transport of solutes towards the membrane by convection and the slower back diffusion of the retained species [32].

3.1.5. Variation of permeate flux

Fig. 6 presents the permeate flux trend as a function of influent salt concentration and applied pressure.

The increase in salt concentration from 1 to 6 g/L resulted in decreased permeate flux from 18 to 12 L/m² h as shown in Fig. 6a. According to van't Hoff equation, at constantly applied pressure, the flux is dependent on the osmotic pressure difference as represented by Eq. (30).

$$\Delta\pi = R_g \times T\left(C_m - C_p\right) \tag{30}$$

According to Eq. (30), the increasing bulk solute concentration leads to the solute concentration on the membrane surface, and thus $C_m - C_p$ increases. Subsequently, the osmotic pressure difference increases. This explains the decrease in flux with the salt concentration in the feed. The same results were reported by Kim et al. [37] decrease in flux was observed with the increased KCl concentration in the feed.

Fig. 6b shows the variation of permeate flux for the NF membrane with the applied pressure variation from 4 to 8 bar. As presented in Fig. 6b, an increase in the applied pressure results in a gradual increase in the permeate flux. The permeate flux of the NF membrane increases from 9.15 to 15.03 L/m² h in line when the applied pressure was increased from 4 to 8 bar. Yuan et al. [40] report the linear increase of the permeate water flux of BTC–TAEA polyamide membrane from 21.5 to 118.6 kg/m² h, when the pressure ranges from 10 to 30 bar.

3.1.6. Modeling

A feed, solution containing 15 mg/L of F⁻, the real and observed rejection of F⁻ with MW: 18.99 g/mol, $D_{i,\infty}$: 1.46 × 10⁻⁹ m²/s [41] and r_s: 0.146 nm are plotted in Fig. 7. The Stokes radius of F⁻ ion was calculated by using the Stokes–Einstein formula [Eq. (31)].

$$D_{i,\infty} = \frac{k_B \times T}{6 \times \pi \times \eta \times r_s} \tag{31}$$

As illustrated in Fig. 7, Eq. (8) fits very well the experimental data. Table 3 lists the estimated parameter values of the solute's rejection model for F⁻ rejection from influent water by the NF membrane.

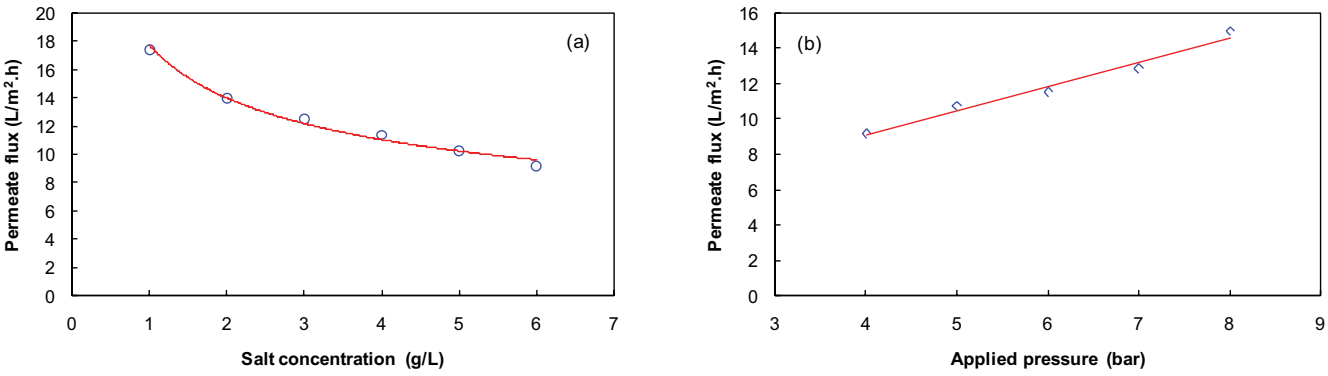

Fig. 6. Variation of permeate flux as a function of (a) influent salt concentration (F⁻ concentration: 15 mg/L, solution pH: 8, and applied pressure: 5 bar) and (b) applied pressure (F⁻ concentration: 15 mg/L, flow rate: 30 L/h, and solution pH: 8).

According to Table 3, the estimated average of pore radius and $\Delta x/A_k$ of the NF membrane are 0.12 ± 0.02 nm and 47.84 ± 25.22 mm, respectively. Cuartas-Uribe et al. [42] operated NF200 and desal 5 DL nanofiltration membranes for lactose rejection and an estimated pore radius of NF200 membrane was observed to be 0.41 nm. In addition, Gherasim et al. [22] reported the r_p and $\Delta x/A_k$ values as 0.26 ± 0.003 nm and 6.33 ± 0.02 mm, respectively, by a rejection of glycerol. The differences between these values and our values for pore radius can be explained probably by assuming some differences between the membrane batches.

To determine the separation mechanism of F^- by NF, the obtained experimental data were fitted with the Spiegler–Kedem model by using the "Solver" analysis function in the "Data Tools" menu in Microsoft Excel 2010. Fig. 8 depicts obtained experimental and predicted data.

As seen in Fig. 8, the Spiegler–Kedem model and constant parameters provided satisfactory predictions of F^- rejection observations. As summarized in Table 4, during F^- rejection by NF, the reflection coefficients were very high (close to 1) and the permeability coefficients were very small. High reflection coefficients indicates convective transport in NF membrane is almost totally sterically hindered [22]. The reflection coefficients for the AFC 40 tubular NF membrane was determined by Gherasim et al. [32] and found to be in the range of 0.79–0.95.

3.2. Binary solution

3.2.1. Influence of co-existing cations

The Na^+ and Ca^{2+} concentration in feed water was increased from 1 to 6 g/L to inspect the influence of co-existing cations on F^- rejection by NF membrane. Fig. 9 reveals the effect of co-existing cation on F^- rejection in respect of co-existing cations concentration and type.

As shown in Fig. 9, the F^- retention was observed to decrease in the presence of co-existing cations. When concentration of co-existing cations in feed water was increased from 0 to 6 g/L, the F^- rejection declined from 96.3% to 60.1% for Na^+ and 96.3% to 48.1% for Ca^{2+}. This behavior is related to shielding of the negatively charged groups on the membrane by cations at high salt concentration and, therefore anions can readily pass through the membrane [34,43]. Nasr et al. [20] showed decrease in F^- retention in the presence of calcium and reached to 66.8% at 200 mg/L of Ca^{2+} concentration. In addition, regarding the salt nature includes cation valency and ionic radius, Ca^{2+} gives the highest influence on F^- retention, followed by Na^+. The decrease in F^- retention with the increase co-existing cations concentration is explained by the membrane charge neutralizing effect [20,34].

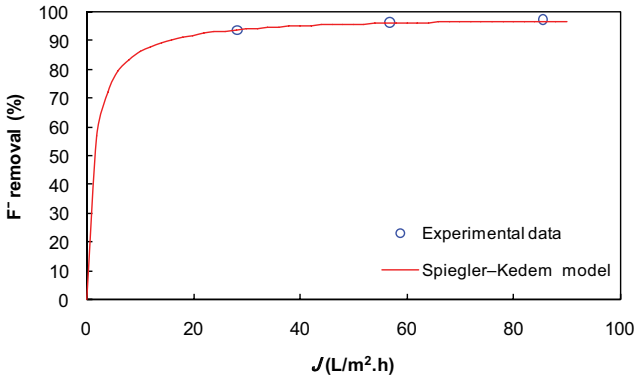

Fig. 8. Experimental data fitting with the Spiegler–Kedem model.

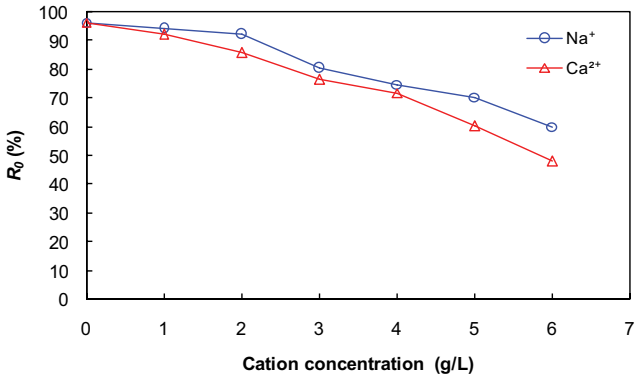

Fig. 9. Influence of cations type and concentration on retention of F^- (F^- concentration: 15 mg/L, solution pH: 8, and applied pressure: 5 bar).

Table 3
Structural parameters of NF90 membrane

F^- concentration (mg/L)	Solution pH	Applied pressure (bar)	Membrane structural parameters		r^2
			r_p (nm)	$\Delta x/A_k$ (mm)	
15	8	5	0.12 ± 0.02	47.84 ± 25.22	0.99

Table 4
Spiegler–Kedem model constants

F^- concentration (mg/L)	Solution pH	Applied pressure (bar)	Spiegler–Kedem model parameters		r^2
			σ (–)	ω (L/m² h)	
15	8	5	0.98	1.44	0.99

3.2.2. Presence of co-existing anion

To evaluate the effectiveness of the NF system developed for a different potential situation, the NF experiments were carried out with different type and concentration of co-existing anions. At these experiments, the F^- concentration of feed water was equal to 15 mg/L. The effect of type and concentration of co-existing anions on the F^- rejection efficiency of NF membrane is shown in Fig. 10.

As illustrated in Fig. 10, the retention of F^- was 96.26% with the NF membrane when F^- is the sole chemical in the feed water. As SO_4^{2-} and PO_4^{3-} was added in steps from 1 to 6 g/L in to feed water, the F^- rejection decreased from 83.87% to 46.39% for SO_4^{2-} and also from 75.89% to 39.72% in case of PO_4^{3-}. When SO_4^{2-} and PO_4^{3-} are added in feed water, to match the Na^+ ions in permeate, more F^- ions than SO_4^{2-} and PO_4^{3-} ions cross the NF membrane and lead to decrease in F^- retention. That is understood as the classical Donnan equilibrium [44]. When comparing between SO_4^{2-} and PO_4^{3-} as co-existing anions, the F^- transport with PO_4^{3-} was somewhat increased. This can be explained by the high affinity of the ionized sites of the membrane increasing the diffusion of salt from the more to the less concentrated solution. Nasr et al. [20] found that in the presence of SO_4^{2-} ions (1 g/L), F^- retention decreases to 61%.

3.3. Evaluation of NF economic

The economic evaluation of the cost of a produced cubic meter requires the calculation of the investment cost and the operating cost. These parameters are determined from the membrane surface, the flow rate, the recovery rate, the velocity in cells, and the outlet concentrations. Table 5 summarized design criteria considered to the construction of economic evolution.

Table 6 was summarized the total annualized cost of the NF process.

As summarized in Table 6, the total annualized cost of water treatment by the NF membrane was calculated to be 0.43 \$/m^3. According to the previous study reports, total operating costs of drinking water production and phenol rejection from coke oven wastewater is 0.38 and 0.46 \$/m^3 of produced water, respectively [29,45]. In addition,

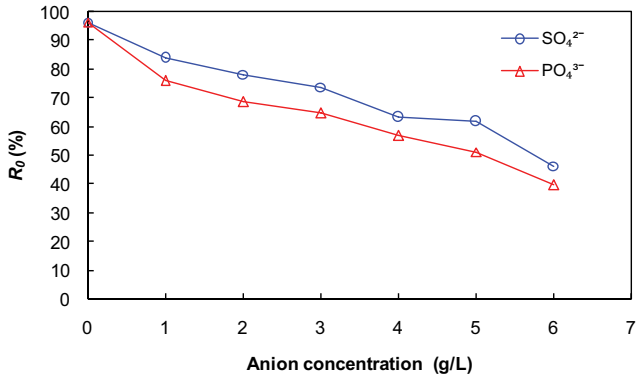

Fig. 10. F^- rejection efficiency as a function of type and concentration co-existing anion (F^- concentration: 15 mg/L, solution pH: 8, and applied pressure: 5 bar).

Table 5
Design criteria for economic evolution

Item	Value
Plant capacity, m^3/h	100
F^- concentration of feed water, mg/L	5
Require F^- rejection efficiency, %	75
Permeate recovery rate, %	30
Operating pressure, bar	8
Membrane flux, m^3/m^2 h	0.12
Membrane module area, m^2	0.5
Project life, y	20
Interest rate, %	15

Table 6
Economical data of NF process

Cost type	Sub-cost	Value (\$)
Investment	(1) Civil	168,183.9 \$
	(2) Mechanical engineering	130,991.6 \$
	(3) Electrical	6,921.4 \$
	(4) Membrane module	1,326,450 \$
	Total capital cost	1,632,546.9 \$
Operating	(5) Maintenance cost	32,650.9 \$
	(6) Membrane	100,000 \$
	(7) Labor	4,800 \$
	Total operating cost	137,450.9 \$
CRF		0.16 \$
The annualized capital cost		0.43 \$

Lahnid et al. [30] evaluated the economic of F^- rejection by electrodialysis and demonstrated the total cost including capital and operational cost estimated to 0.36 \$/m^3.

4. Conclusion

This paper investigated the performance of NF90 (thin-film composite NF membrane) in the rejection of F^- ions from model groundwater under various operational conditions, as well as their separation mechanism in correlation with the membrane characteristics. In addition, the economic evaluation of F^- rejection from groundwater was estimated based on actual industrial and economic data. Based on the obtained results, the lower F^- rejection was obtained in solution pH of 5 and the acidic and alkaline solution pH lead to higher F^- rejection. At low solution pH, higher F^- rejection was related to higher osmotic pressure near the membrane surface. Ion concentration had a positive effect and the F^- transmittance increased with the increasing concentration on the feed phase because of membrane charges neutralization. The permeate flux was enhanced and the F^- rejection was improved by increasing the crossflow velocity, which diminishes the concentration polarization phenomenon. Furthermore, it was observed, comparing with SO_4^{2-}, the presence of PO_4^{3-} as a co-existing anion in feed water proved to be more effective for F^- transport and could

be explained by the classical Donnan equilibrium. Regarding salt nature, Ca^{2+} had the highest influence on F^- retention, followed by Na^+. The membrane characterization study showed the estimated average pore radius and $\Delta x/A_k$ of the NF membrane were 0.12 ± 0.02 nm and 47.84 ± 25.22 mm, respectively. The processes were characterized with high accuracy by the Spiegler–Kedem model, and σ coefficient was observed to be 0.98 which indicates convective transport in the NF membrane is almost totally sterically hindered and revealed that application of a simple model for process prediction is a useful tool for practical NF applications. With the calculation of the capital and the operating costs, the total annualized cost of water treatment by NF was 0.43 \$/m^3.

Symbols

A_k	–	Membrane porosity
$C_{i,f}$	–	F^- concentration in feed water
$C_{i,m}$	–	F^- concentration on membrane surface
$C_{i,p}$	–	F^- concentration in permeate
d_h	–	Hydraulic diameter of membrane channel
$D_{i,\infty}$	–	Solute bulk diffusivity
$H(\lambda_i)$	–	Diffusion
J_p	–	Permeate flux
J_w	–	Pure water flux
k_B	–	Boltzmann constant (1.38e^{-23} J/K)
$K_{i,c}$	–	Convection hindrance factor
$K_{i,d}$	–	Diffusion hindrance factor
L_p	–	Pure water permeability
Pe	–	Peclet number
R	–	Intrinsic (real) rejection
R_g	–	Molar gas constant (8.3144621 J/mol K)
R_0	–	Observed rejections
Re	–	Reynolds number
$r_{i,s}$	–	F^- stokes radius
r_p	–	Pore radius
Sc	–	Schmidt number
Sh	–	Sherwood number
T	–	absolute temperature
u	–	Fluid velocity in membrane channel
$W(\lambda_i)$	–	Convection
x	–	Distance in membrane
ΔP	–	Transmembrane pressure
Δx	–	Effective membrane thickness
η	–	Dynamic viscosity of aqueous solution
λ_i	–	Ratio of F^- to pore size
ϱ	–	Density of aqueous solution
σ	–	Reflection coefficient
Φ_i	–	Solute steric partitioning coefficient
ω	–	Solute permeability

Acknowledgments

The authors thank the Student Research committee of Isfahan University of Medical Sciences of Iran (Project No. 197104 and Ethics code: IR.MUI.RESEARCH.REC.1397.241) for financial support of this work.

References

[1] WHO, Guidelines for Drinking-Water Quality, World Health Organization, Geneva, 2004.
[2] S. Erdal, S.N. Buchanan, A quantitative look at fluorosis, fluoride exposure, and intake in children using a health risk assessment approach, Environ. Health Perspect., 113 (2004) 111–117.
[3] A. Bhatnagar, E. Kumar, M. Sillanpää, Fluoride removal from water by adsorption-a review, Chem. Eng. J., 171 (2011) 811–840.
[4] S. Aghapour, B. Bina, M.J. Tarrahi, F. Amiri, A. Ebrahimi, Distribution and health risk assessment of natural fluoride of drinking groundwater resources of Isfahan, Iran, using GIS, Environ. Monit. Assess., 190 (2018) 137.
[5] J. Doull, K. Boekelheide, B. Farishian, R. Isaacson, J. Klotz, J. Kumar, H. Limeback, C. Poole, J. Puzas, N. Reed, Fluoride in Drinking Water: A Scientific Review of EPA's Standards, National Academies, Washington, DC, 2006, pp. 205–223.
[6] H. Biglari, A. Chavoshani, N. Javan, A. Hossein Mahvi, Geochemical study of groundwater conditions with special emphasis on fluoride concentration, Iran, Desal. Water Treat., 57 (2016) 22392–22399.
[7] M.R. Mohebbi, R. Saeedi, A. Montazeri, K. Azam Vaghefi, S. Labbafi, S. Oktaie, M. Abtahi, A. Mohagheghian, Assessment of water quality in groundwater resources of Iran using a modified drinking water quality index (DWQI), Ecol. Indic., 30 (2013) 28–34.
[8] H. Amini, G.A. Haghighat, M. Yunesian, R. Nabizadeh, A.H. Mahvi, M.H. Dehghani, R. Davani, A.-R. Aminian, M. Shamsipour, N. Hassanzadeh, Spatial and temporal variability of fluoride concentrations in groundwater resources of Larestan and Gerash regions in Iran from 2003 to 2010, Environ. Geochem. Health, 38 (2016) 25–37.
[9] M. Mirzabeygi Rad Fard, M. Yousefi, H. Soleimani, A.A. Mohammadi, A.H. Mahvi, A. Abbasnia, The concentration data of fluoride and health risk assessment in drinking water in the Ardakan city of Yazd province, Iran, Data Brief, 18 (2018) 40–46.
[10] S.S. Waghmare, T. Arfin, Fluoride removal from water by various techniques, Int. J. Innovative Sci. Eng. Technol., 2 (2015) 560–571.
[11] Meenakshi, R.C. Maheshwari, Fluoride in drinking water and its removal, J. Hazard. Mater., 137 (2006) 456–463.
[12] I. Ali, V. Gupta, Advances in water treatment by adsorption technology, Nat. Protoc., 1 (2006) 2661–2667.
[13] M. Tahaikt, R. El Habbani, A. Ait Haddou, I. Achary, Z. Amor, M. Taky, A. Alami, A. Boughriba, M. Hafsi, A. Elmidaoui, Fluoride removal from groundwater by nanofiltration, Desalination, 212 (2007) 46–53.
[14] B. Van der Bruggen, C. Vandecasteele, Removal of pollutants from surface water and groundwater by nanofiltration: overview of possible applications in the drinking water industry, Environ. Pollut., 122 (2003) 435–445.
[15] K. Hu, J.M. Dickson, Nanofiltration membrane performance on fluoride removal from water, J. Membr. Sci., 279 (2006) 529–538.
[16] S. Chakrabortty, M. Roy, P. Pal, Removal of fluoride from contaminated groundwater by cross flow nanofiltration: transport modeling and economic evaluation, Desalination, 313 (2013) 115–124.
[17] R. Malaisamy, A. Talla-Nwafo, K.L. Jones, Polyelectrolyte modification of nanofiltration membrane for selective removal of monovalent anions, Sep. Purif. Technol., 77 (2011) 367–374.
[18] S.V. Jadhav, K.V. Marathe, V.K. Rathod, A pilot scale concurrent removal of fluoride, arsenic, sulfate and nitrate by using nanofiltration: competing ion interaction and modelling approach, J. Water Process Eng., 13 (2016) 153–167.
[19] M. Tahaikt, A. Ait Haddou, R. El Habbani, Z. Amor, F. Elhannouni, M. Taky, M. Kharif, A. Boughriba, M. Hafsi, A. Elmidaoui, Comparison of the performances of three commercial membranes in fluoride removal by nanofiltration. Continuous operations, Desalination, 225 (2008) 209–219.
[20] A.B. Nasr, C. Charcosset, R.B. Amar, K. Walha, Defluoridation of water by nanofiltration, J. Fluorine Chem., 150 (2013) 92–97.
[21] J. Hoinkis, S. Valero-Freitag, M.P. Caporgno, C. Pätzold, Removal of nitrate and fluoride by nanofiltration – a comparative study, Desal. Water Treat., 30 (2011) 278–288.

[22] C.-V. Gherasim, J. Cuhorka, P. Mikulášek, Analysis of lead(II) retention from single salt and binary aqueous solutions by a polyamide nanofiltration membrane: experimental results and modelling, J. Membr. Sci., 436 (2013) 132–144.
[23] M.M. Zerafat, M. Shariati-Niassar, S.J. Hashemi, S. Sabbaghi, A.F. Ismail, T. Matsuura, Mathematical modeling of nanofiltration for concentrated electrolyte solutions, Desalination, 320 (2013) 17–23.
[24] R.B. Baird, A.D. Eaton, E.W. Rice, Standard Methods for the Examination of Water and Wastewater, 23rd ed., AWWA, WEF and APHA, Washington DC, USA, 2017.
[25] R.G. Deissler, Analysis of Turbulent Heat Transfer, Mass Transfer, and Friction in Smooth Tubes at High Prandtl and Schmidt Numbers, National Advisory Committee for Aeronautics (NACA), Technical Note: 3145, Washington, DC, USA, 1954.
[26] A.I. Cavaco Morão, A. Szymczyk, P. Fievet, A.M. Brites Alves, Modelling the separation by nanofiltration of a multi-ionic solution relevant to an industrial process, J. Membr. Sci., 322 (2008) 320–330.
[27] P. Dechadilok, W.M. Deen, Hindrance factors for diffusion and convection in pores, Ind. Eng. Chem. Res., 45 (2006) 6953–6959.
[28] K.S. Spiegler, O. Kedem, Thermodynamics of hyperfiltration (reverse osmosis): criteria for efficient membranes, Desalination, 1 (1966) 311–326.
[29] A. Verberne, J. Wouters, Membraanfiltratie voor de drinkwater bereiding: economische optimalisatie van ontwerpparameters, H_2O, 26 (1993) 383–387.
[30] S. Lahnid, M. Tahaikt, K. Elaroui, I. Idrissi, M. Hafsi, I. Laaziz, Z. Amor, F. Tiyal, A. Elmidaoui, Economic evaluation of fluoride removal by electrodialysis, Desalination, 230 (2008) 213–219.
[31] A.E. Childress, M. Elimelech, Relating nanofiltration membrane performance to membrane charge (electrokinetic) characteristics, Environ. Sci. Technol., 34 (2000) 3710–3716.
[32] C.-V. Gherasim, K. Hancková, J. Palarčík, P. Mikulášek, Investigation of cobalt(II) retention from aqueous solutions by a polyamide nanofiltration membrane, J. Membr. Sci., 490 (2015) 46–56.
[33] G. Hagmeyer, R. Gimbel, Modelling the rejection of nanofiltration membranes using zeta potential measurements, Sep. Purif. Technol., 15 (1999) 19–30.
[34] A.H. Mahvi, M. Malakootian, A. Fatehizadeh, M.H. Ehrampoush, Nitrate removal from aqueous solutions by nanofiltration, Desal. Water Treat., 29 (2011) 326–330.
[35] N. Yousefi, A. Fatehizedeh, K. Ghadiri, N. Mirzaei, S.D. Ashrafi, A.H. Mahvi, Application of nanofilter in removal of phosphate, fluoride and nitrite from groundwater, Desal. Water Treat., 57 (2016) 11782–11788.
[36] F. Garcia, D. Ciceron, A. Saboni, S. Alexandrova, Nitrate ions elimination from drinking water by nanofiltration: membrane choice, Sep. Purif. Technol., 52 (2006) 196–200.
[37] H.H. Kim, J.H. Kim, Y.K. Chang, Removal of potassium chloride by nanofiltration from ion-exchanged solution containing potassium clavulanate, Bioprocess. Biosyst. Eng., 33 (2010) 149–158.
[38] A. Werner, A. Rieger, K. Helbig, B. Brix, J. Zocher, R. Haseneder, J.-U. Repke, Nanofiltration for the recovery of indium and germanium from bioleaching solutions, Sep. Purif. Technol., 224 (2019) 543–552.
[39] B. Gonzalez, S.G.J. Heijman, L.C. Rietveld, D. van Halem, Arsenic removal from geothermal influenced groundwater with low pressure NF pilot plant for drinking water production in Nicaraguan rural communities, Sci. Total Environ., 667 (2019) 297–305.
[40] B. Yuan, P. Li, P. Wang, H. Yang, H. Sun, P. Li, H. Sun, Q.J. Niu, Novel aliphatic polyamide membrane with high mono-/divalent ion selectivity, excellent Ca^{2+}, Mg^{2+} rejection, and improved antifouling properties, Sep. Purif. Technol., 224 (2019) 443–455.
[41] P. Vanysek, Ionic conductivity and diffusion at infinite dilution, CRC Handb. Chem. Phys., 83 (2000) 76–78.
[42] B. Cuartas-Uribe, M. Vincent-Vela, S. Álvarez-Blanco, M. Alcaina-Miranda, E. Soriano-Costa, Nanofiltration of sweet whey and prediction of lactose retention as a function of permeate flux using the Kedem–Spiegler and Donnan Steric Partioning models, Sep. Purif. Technol., 56 (2007) 38–46.
[43] A. Fatehizadeha, E. Taheria, M.M. Amina, M. Mahdavid, N. Moradia, Sodium and potassium removal from brackish water by nanofiltration membrane: single and binary salt mixtures, Desal. Water Treat., 103 (2018) 65–71.
[44] F. Durmaz, H. Kara, Y. Cengeloglu, M. Ersoz, Fluoride removal by Donnan dialysis with anion exchange membranes, Desalination, 177 (2005) 51–57.
[45] R. Kumar, P. Pal, Removal of phenol from coke-oven wastewater by cross-flow nanofiltration membranes, Water Environ. Res., 85 (2013) 447–455.